The generation of 1.2 μJ pulses from a Mamyshev oscillator based on a high concentration, large-mode-area Yb-doped fiber

Di Lin, Duangyang Xu, Jing He, Yutong Feng, Zhengqi Ren, Raghuraman Sidharthan, Yongmin Jung, *Senior Member, IEEE*, Seongwoo Yoo, David J. Richardson, *Fellow, IEEE*

***Abstract*— We demonstrate a high-energy and high-average power Mamyshev oscillator based on a high performance large-mode-area step-index germanosilicate-cladding Yb-doped fiber. The oscillation of higher-order modes is effectively suppressed by employing appropriate intracavity spatial mode filtering, allowing significant scaling of single pulse energy. The laser directly generates a nearly diffraction-limited beam with an average power of 17 W operating at the fundamental repetition rate of 14.01 MHz, corresponding to a pulse energy of 1.2 μJ. The pulses could be externally dechirped to ~58 fs, leading to a peak power of ~13 MW. To the best of our knowledge, this is the highest pulse energy with sub-100 fs duration ever obtained directly from a mode-locked fiber oscillator.**

***Index Terms*— Mode locked fiber oscillator, Ultrafast pulses.**

I. Introduction

High-peak power femtosecond fiber lasers are gaining attraction within a wide range of industrial and scientific applications, including material processing [1, 2] and nonlinear microscopy [3, 4] due to their efficiency, compactness, robustness, and relatively low cost. Furthermore, because of their excellent heat dissipation and the tight confinement of light in the fiber core, they are suitable for high-average power operation while maintaining good beam quality. However, the tight optical confinement causes strong nonlinear effects, limiting the maximum pulse energy well below that possible from their bulk solid-state counterparts. Early soliton fiber lasers could only produce pulses with an energy of a few hundred pJ [5]. However, over the past few decades, substantial efforts have been devoted to managing the nonlinearity in order to increase the pulse energy, resulting in the development of novel cavity concepts and designs including stretched-fiber lasers [6], self-similar fiber lasers [7] and all-normal dispersion (ANDi) fiber lasers [8]. Such laser configurations can typically generate sub-100 fs pulses with nJ - level pulse energy from single-mode fibers (SMFs) by employing saturable absorbers (SAs) with a high modulation depth such as nonlinear polarization evolution (NPE) [9], semiconductors mirrors [10], and nonlinear amplifying fiber loop mirrors [11].

Recently, the Mamyshev oscillator (MO) based on self-phase modulation (SPM) induced spectral broadening and subsequent offset spectral filtering has attracted rapidly growing attention owing to its outstanding performance in terms of pulse energy, pulse duration, and environmental stability. The first compelling demonstration of the energy scaling benefits of the MO approach led to the generation ~50 nJ pulses with a pulse duration of ~40 fs using a 6 μm core diameter step-index polarization-maintaining (PM) single-mode Yb-doped fiber (YDF) [12]. A straightforward way to further scale the pulse energy is by employing fibers with larger cores so that an increase in pulse energy can be obtained whilst maintaining the accumulated nonlinear phase shift at the levels needed to avoid pulse breakup. In this way, ~190 nJ pulse energy was achieved in a MO using an essentially SMF with a core diameter of 10 μm [13], and the pulse energy was further scaled to ~1.1 μJ using a large-core photonic-crystal fiber (PCF) capable of effective single-mode operation. However, the use of PCFs brings some practical issues in terms of high cost, high bend sensitivity, and difficult integration into all-fiber format systems. On the other hand, standard step-index large-core fibers can in part address these issues, however the presence of higher-order modes as typically supported in such fibers, can significantly disrupt the mode-locking. The

Manuscript received March 20, 2022; revised June 25; accepted July 30. This work was supported in part by the UK EPSRC funded "Airguide Photonics" programme grant (EP/P030181/1), in part by the EPSRC funded "National Hub in High Value Photonic Manufacturing" grant (EP/N00762X/1), and in part by EPSRC funded "Laser Technology for Future Manufacturing" platform grant (EP/P027644/1) *(Corresponding author: Di Lin, Zhengqi Ren).*

Di Lin, Duanyang Xu, Yutong Feng, Zhengqi Ren, Yongmin Jung, and David J. Richardson are with Optoelectronics Research Centre, University of Southampton, Southampton, SO17 1BJ, UK (e-mail: dilin@gdut.edu.cn; dx1a17@soton.ac.uk; ytfeng@outlook.com; zr2y14@soton.ac.uk; ymj@orc.soton.ac.uk; djr@orc.soton.ac.uk). Di Lin is now with the School of Information Engineering and Guangdong Provincial Key Laboratory of Photonics Information Technology, Guangdong University of Technology, Guangzhou, 510006, China.

Jing He is with Cambridge Graphene Centre, University of Cambridge, CB3 0FA, UK (e-mail: jh2179@cam.ac.uk).

Raghuraman Sidharthan and Seongwoo Yoo are with School of Electrical and Electronic Engineering, COFT, TPI, Nanyang Technological University, 50 Nanyang Avenue 639798, Singapore (e-mail: sidearthan@ntu.edu.sg; seon.yoo@ntu.edu.sg).

Color versions of one or more of the figures in this article are available online at http://ieeexplore.ieee.org

Digital Object Identifier

increasing difficulty of suppressing higher order mode content as the core size is increased eventually limits the maximum achievable pulse energy [14].

Here, we report on the generation of femtosecond pulses from a MO based on the use of a high performance in-house fabricated step-index YDF with a large core diameter of ~33 µm. A germanium (Ge)-doped cladding is employed to offset the high refractive index associated with the high Yb concentration in the fiber core, resulting in an ultra-low numerical aperture (NA) of ~0.042 that favors LP_{01} mode operation with a large mode area (LMA) of ~540 µm^2. Any potentially adverse effects of higher-order modes on the mode-locking were further mitigated by appropriate intracavity spatial mode filtering. The fiber provides a high cladding absorption of > 20 dB/m at 975 nm, which is at least ~ 1.5 times higher than commercially available Yb-doped LMA PCF. This allows a high gain from a very short length of fiber as needed to help increase the threshold for nonlinear effects during amplification of the circulating pulses. The MO reaches 17 W of average power at a repetition rate of 14.01 MHz, corresponding to 1.2 µJ pulses. The output pulses are dechirped down to ~58 fs with ~13 MW peak power external to the cavity. To the best of our knowledge, this is the highest single-pulse energy ever obtained directly from a mode-locked fiber oscillator.

II. Experimental Setup

Fig. 1 shows a schematic of the experimental setup. It comprises two cascaded Mamyshev fiber regenerators/amplifiers. The first regenerator consists of a ~2.5-m length of PM-YDF (Nufern PLMA-YDF-25/250-VIII) with a core/cladding diameter of 25/250 µm and an NA of 0.065/0.46, respectively. The V-number of the fiber core around 1.04 µm is ~5.1 indicating that the fiber is able to support higher-order mode propagation up to the LP_{02} mode. The fiber was tightly coiled with a bending diameter of ~7 cm thereby inducing high losses for all higher-order modes whilst at the same time resulting in minimal additional loss for the fundamental LP_{01} mode. In this way the fiber operates effectively as an SMF by suppressing the propagation of higher-order modes. The first regenerator acts as a lower-energy amplifier for the second power scaling regenerator and is forward cladding-pumped with a multimode 975 nm pigtailed laser diode via a pump/signal combiner. The output port of the combiner has a matched passive fiber to the gain fiber, and the signal input port of the combiner is effectively SMF with a core diameter of 10 µm and an NA of 0.085. A tapered mode field adapter is integrated within the combiner to favor the excitation of the fundamental LP_{01} mode at the output port which was spliced to the PM-YDF. A 10dB SMF tap (2×2 ports) is spliced to the signal input port of the pump/signal combiner, which is used for coupling both the circulated pulses from the power-scaling regenerator and the externally injected seed needed to initiate the mode-locking. A free-space thin-film bandpass filter (Semrock, LL01-1064-25) with a center wavelength set at 1046 nm and a bandwidth of 4 nm full-width at half-maximum (FWHM) is placed after the output coupler of the first arm. The

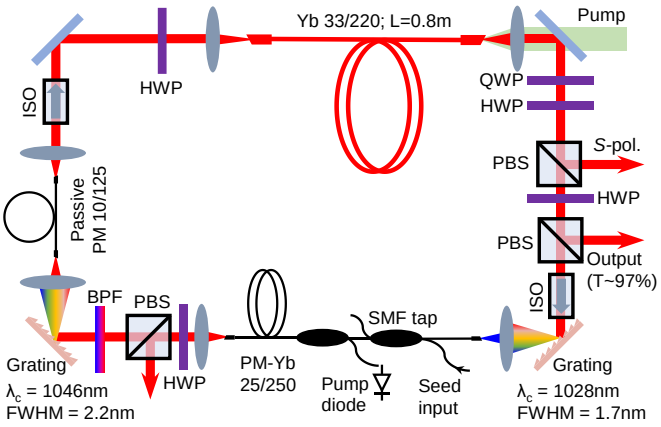

Fig. 1 Schematic of the experimental setup. HWP: half-wave plate; ISO: isolator; PBS: polarization beam splitter; QWP: quarter-wave plate; T: transmittance; S-pol.: S-polarization.

main purpose of the filter is to further reduce the backward propagating amplified spontaneous emission (ASE) around 1030 nm and to suppress parasitic lasing around the peak wavelength of the ASE.

The second regenerator consists of a ~0.8-m length of in-house-made LMA step-index non-PM YDF with Ge-doped cladding that has a core diameter of 33 µm with an ultra-low NA of 0.042 and a cladding diameter of 220 µm [15]. The V-number is calculated to be ~4.2 at 1.04 µm. As the fiber is short, it was loosely coiled with a bend diameter of ~16 cm with just 1 turn. A numerical calculation (using the COMSOL Finite Element Method software package) shows that the effective mode area of the LP_{01} mode decreases from ~650 µm^2 (straight fiber) to 540 µm^2 in the coiled case and the other higher-order modes are cut-off. The fiber cladding absorption at 975 nm was measured to be ~22 dB/m using the cutback method. Compared to conventional YDFs, the higher pump absorption coefficient allows for much shorter fiber lengths, reducing the nonlinear phase shift and thus allowing for pulse energy scaling. The fiber is backward cladding-pumped with a 975nm pump module via a lens and dichroic mirror assembly. All fiber ends of the YDFs were spliced to appropriate silica endcaps with a diameter of ~250 µm and these were polished with an angle of ~8 degree to suppress the potential for parasitic lasing.

Two free-space polarization independent isolators ensure unidirectional (clockwise) operation and aid in the suppression of parasitic lasing due to potential residual back reflections from the fiber ends. Both isolators were aligned with a small angle with respect to the optical axis in order to reduce the feedback of residual back reflections caused by the input and output surfaces of the isolators themselves. The offset bandpass filters are formed by two reflective ruled diffractive gratings (Thorlabs, GR25-0303) with groove densities of 300 lines/mm in combination with SMF coupling fibers, each offering Gaussian-shaped spectral transmission profiles – one with a center wavelength set at 1046 nm with a 2.2 nm FWHM, and the other at 1028 nm with 1.7 nm FWHM. The differences in bandwidth of the spectral filters were achieved by varying the beam size of the collimated beam incident on the grating. The

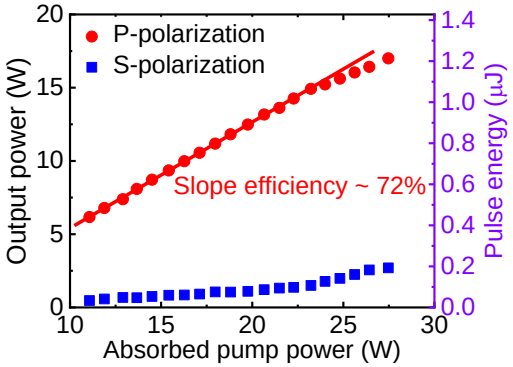

Fig. 2 The averaged output power and pulse energy as a function of absorbed pump power.

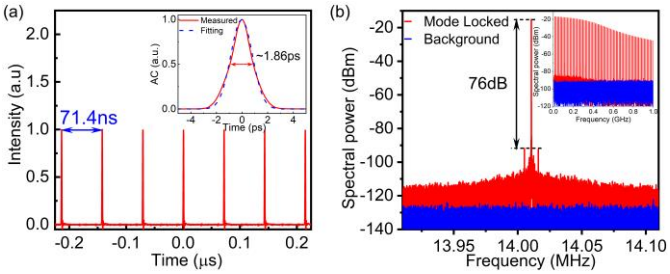

Fig. 3 (a)Oscilloscope trace of the output pules. Inset: autocorrelation trace of the output pulses. (b)RF spectrum with a RBW of 10Hz and a span of 200kHz at the fundamental frequency of 14.01MHz. Inset: RF spectrum with 1GHz span.

large spectral separation between the two filters results in a high modulation depth for the effective saturable absorber, allowing high energy pulses to be stabilized. The two SMFs (one with a core diameter of 10 μm and the other with a core diameter of 6 μm) placed behind the gratings also form two intracavity spatial-mode filters that further suppress the oscillation of higher-order modes. This is critical for realizing the full pulse energy scaling potential of the few-mode LMA fiber as mode-locking can be significantly disrupted by the presence of high-order modes and result in much lower maximum single-pulse energies [14]. The total length of fiber used is ~5 m, and the beam emitted from the 10 μm passive fiber is collimated and propagated through a ~12-m length in free-space so that the fundamental repetition rate of the oscillator is reduced to ~14.01 MHz to accommodate the available pump power to the anticipated circulating pulse energy. The combination of the HWP and the PBS in each arm forms an adjustable output coupler. We minimized the output coupling ratio in the first arm to ensure that the signal power seeded into the second arm is as high as possible to reduce the gain burden on the second arm which reduces the ASE and again helps to suppress parasitic lasing, while the output coupling ratio of the second arm was set to ~97% to maximize the energy of the output pulses. Note that a combination of a QWP and a HWP is placed after the fiber output to compensate for any depolarization in the output beams emitted from the non-PM-YDF. Any residual S-polarized component is separated by the PBS placed before the output coupler.

III. Results and Discussion

We employed a home-made, dispersion-managed mode-locked fiber oscillator to provide an external signal to start the mode-locking. It operates at a repetition rate of 23.15 MHz and has a center spectral wavelength of 1038 nm. The output pulses are first compressed to ~300 fs before passing through a 2-m length of SMF to increase the spectral bandwidth to ~30 nm, which spans the passbands of the two intracavity spectral filters. Mode-locking of the MO could be repeatably started within the single pulse regime at a fundamental repetition rate of 14.01 MHz by properly aligning the ring cavity, increasing the absorbed pump power in the second arm to ~11.5W, and adjusting the energy of the seed pulses launched in to the first arm to ~5 pJ. Multi-pulsing and higher-order harmonic operation, frequently encountered in such lasers, was not observed during the process of initiating the mode-locking [16]. This is primarily due to the relatively high intracavity loss caused by the high output coupling ratio of the second arm (~97%), as well as the high modulation depth of the saturable absorber induced by the large separation of the center wavelength for the two spectral filters. It should be noted that a seed with too high a pulse energy would result in seed amplification, while a seed with too low a pulse energy would not allow for sufficient spectral broadening to enable pulses to circulate through the two cascaded regenerators. Once the mode-locking has been initiated, blocking the seed pulses helps the oscillator operate more stably. We observed that a slight decrease in pump power close to the threshold in the second arm would lead to a sudden loss of mode-locking. In the case of our optimum start parameters, the minimum output power of the oscillator is ~6W, corresponding to a pulse energy of ~428 nJ. We then gradually increased the pump power in the second arm to increase the output power of the MO. Fig. 2 depicts the average output power and associated pulse energy of the mode-locked pulses as a function of absorbed pump power. The average output power reaches a maximum of 17 W with a slope efficiency of ~72% with respect to the absorbed pump power. It is worth mentioning that the pump power of the first arm was kept constant, resulting in a nearly constant power of ~27 mW (~1.9 nJ) of signal that could be seeded into the power scaling arm. Taking 1 dB of signal coupling loss into account, the second arm provides an effective gain of ~29 dB, reaching a maximum single-pulse energy of ~1.2 μJ. Note that the orientations of the fast axis of the QWP and HWP before the first PBS and the HWP before the LMA non-PM YDF must be slightly rotated to maintain maximum polarization extinction ratio (PER) for the output beam (measured by the ratio of the output to the s-polarization power) as the pump power is increased. We observed that the output power exhibits a slight roll-off above 15 W with a rapid increase of output power for the s-polarization component, and the PER decreases from 11 dB to 8 dB at the maximum 17 W. This might be due to the rapid buildup of ASE caused by the high gain operation, as well as strong nonlinear polarization evolution.

Fig. 3(a) depicts the output pulse train in the electrical domain at a pulse energy of 1.2 μJ. It has a period of ~71.4 ns, corresponding to a repetition rate of ~14.01 MHz, which is in agreement with the calculation based on the cavity length. No satellite pulse is observed between consecutive pulses. The

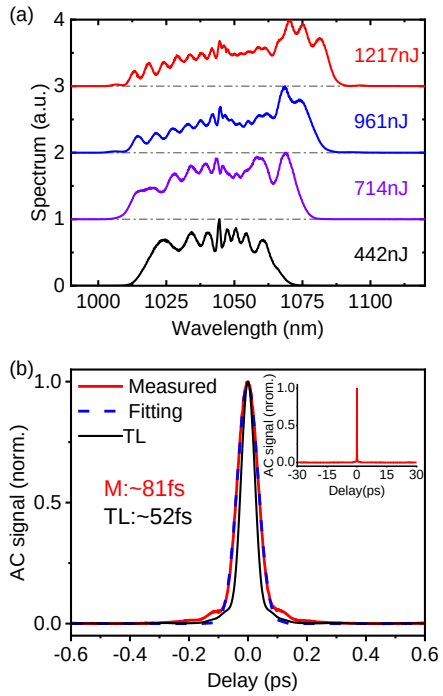

Fig. 4 (a) Experimental spectrum with increasing pulse energy. (b) The measured intensity AC trace (red curve) of the compressed pulse at the maximum pulse energy of 1.2 µJ and the comparison with a Gaussian-fit (blue dash curve) and the calculated AC trace of the transform-limited (TL) pulse (black curve). Inset: 60 ps span.

duration of the intensity autocorrelation (AC) trace for the chirped output pulses was measured to be ~1.86 ps as shown in the inset of Fig. 3(a) in red curves. It infers a pulse duration of ~1.32 ps assuming a Gaussian-shaped pulse, resulting in a peak power of ~ 900 kW for the chirped output pulses. The stability of the output pulse train was further investigated using a radio-frequency (RF) spectrum analyzer. As shown in Fig. 3(b), the fundamental beat mode is measured at a center frequency of ~14.01 MHz with a span window of 200 kHz and a 10 Hz resolution bandwidth (RBW). The linewidth of the RF spectrum(FWHM) is measured to be as narrow as ~30 Hz with a contrast of ~76 dB relative to the secondary modulations, indicating highly stable mode-locking with low pulse jitter. The inset shows the recorded RF spectrum with a span of 1 GHz and a RBW of 10 kHz, showing no sign of multiple pulsing. The stability of the laser operation was confirmed by monitoring the laser over 1-hour of continuous operation. No temporal or spectral deterioration was observed. Fig. 4(a) shows the output spectra directly measured after the output coupler of the second arm for various pulse energies. It shows a typical SPM-broadened spectra for a nearly unchirped Gaussian pulse [17]. The bandwidth at the -10dB level increases from ~54 nm to ~76 nm (ranging from 1011 nm to 1087 nm) as the pulse energy increases from 442 nJ to 1217 nJ. The bandwidth is much narrower than the results shown in ref. [16] which used PCFs with a core diameter of 32 µm to obtain ~1.1 µJ of pulse energy. This can be attributed to the much weaker nonlinear effects that the pulses experienced due to the shorter length of fiber used. The spectra have asymmetric profiles, owing to the self-steepening effect and pulse distortions caused by third-order dispersion. The output pulses were externally

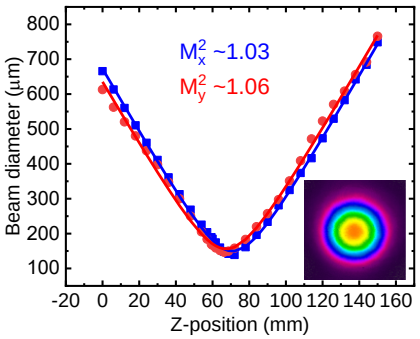

Fig. 5 The measured beam diameter as a function of z-position detuning from the beam waist at the maximum output power. Inset: far-field beam intensity profile.

compressed using a pair of transmission diffraction gratings (1000 lines/mm) with a compression efficiency of ~72%, leading to a maximum compressed pulse energy of ~876 nJ. We observed that the AC durations of the compressed pulses gradually decreased with increasing pulse energy due to the progressively broadened spectrum. The duration of the AC trace of the compressed pulse was measured to be ~81 fs (FWHM) at the maximum pulse energy, as shown in the red curves in Fig. 4 (b). It is reasonably well fitted with an AC trace for a Gaussian-shaped pulse as shown in the blue-dash curves, indicating that the incident Gaussian-shaped pulse has not evolved to a substantially parabolic shape as shown in ref. [12] due to the much shorter length of fiber used in our case. The AC trace clearly has a low pedestal, and through integration we infer that the main lobe contains ~90% of the total energy. As shown in the black curve, the calculated TL pulse has an AC duration of ~52 fs, which is ~1.56 times shorter than the measured pulse. Assuming a Gaussian pulse shape, the temporal duration of the compressed pulse is estimated to be ~58 fs, resulting in a peak power of ~13.6 MW. The deviation between the measured and the TL AC duration can be attributed to higher order phase caused by nonlinear effects and the grating compressor itself. The clean and single AC trace peak measured with a long range delay window of 60ps, as shown in the inset of Fig. 4 (b), excludes any broad pedestal underneath the signal and potential existence of multiple pulses.

The output beams maintain good beam quality above the mode-locking threshold. Fig. 5 shows the typical measured beam quality (M^2) for compressed pulses at the maximum pulse energy, obtaining a value of M^2 <1.1 on both axes. The far-field intensity profile, as shown in the inset, exhibits a circularly symmetric Gaussian shape, indicating that the higher-order modes are well suppressed.

IV. Conclusion

In conclusion, we have demonstrated a MO using an in-house fabricated LMA step-index germanosilicate-cladding YDF with an ultra-low NA of 0.042 and a high cladding absorption of >20 dB/m in one arm. This enables fundamental LP_{01} mode operation with a large effective mode area of ~540 µm^2 in a very short length of fiber, facilitating the effective reduction of fiber nonlinearities to scale the pulse energy. By appropriately bending the LMA fibers and combining that with the use of SMF-based intracavity spatial filters we were able to avoid

higher-order mode disturbances to the mode-locking and were able to scale the single pulse energy as intended. The oscillator generates a nearly diffraction-limited beam with M^2<1.1 at an average output power of 17 W and a pulse energy of ~1.2 µJ, which can be externally compressed to ~58 fs with a peak power of ~13 MW. This is, so far, the highest pulse energy obtained directly from a mode-locked fiber oscillator. There is great potential to convert this architecture to an all-fiber format MO using conventional step-index LMA fibers, enabling a more compact and stable laser system that should be of interest for many applications requiring high-energy ultrashort pulses.

ACKNOWLEDGMENT

The data for this work is accessible through the University of Southampton Institutional Research Repository (DOI: https://doi.org/10.5258/SOTON/D2284). For the purpose of open access, the authors have applied a creative common attribution (CC BY) license to any author accepted manuscript version arising.

REFERENCES

[1] K. Sugioka and Y. Cheng, "Ultrafast lasers-reliable tools for advanced materials processing," *Light Sci. Appl.*, vol. 3, Apr. 2014.
[2] E. H. Penilla *et al.*, "Ultrafast laser welding of ceramics," *Science*, vol. 365, no. 6455, pp. 803-808, Aug. 2019.
[3] J. Squier and M. Muller, "High resolution nonlinear microscopy: A review of sources and methods for achieving optimal imaging," *Rev. Sci. Instrum.*, vol. 72, no. 7, pp. 2855-2867, Jul. 2001.
[4] R. Carriles *et al.*, "Invited Review Article: Imaging techniques for harmonic and multiphoton absorption fluorescence microscopy," *Rev. Sci. Instrum.*, vol. 80, no. 8, Aug. 2009.
[5] F. W. Wise, A. Chong, and W. H. Renninger, "High-energy femtosecond fiber lasers based on pulse propagation at normal dispersion," *Laser Photonics Rev.*, vol. 2, no. 1-2, pp. 58-73, Apr. 2008.
[6] K. Tamura, E. P. Ippen, H. A. Haus, and L. E. Nelson, "77-fs Pulse Generation from a Stretched-Pulse Mode-Locked All-Fiber Ring Laser," *Opt. Lett.*, vol. 18, no. 13, pp. 1080-1082, Jul. 1993.
[7] F. O. Ilday, J. R. Buckley, W. G. Clark, and F. W. Wise, "Self-similar evolution of parabolic pulses in a laser," *Phys. Rev. Lett.*, vol. 92, no. 21, May 2004.
[8] A. Chong, J. Buckley, W. Renninger, and F. Wise, "All-normal-dispersion femtosecond fiber laser," *Opt. Express*, vol. 14, no. 21, pp. 10095-10100, Oct. 2006.
[9] V. J. Matsas, T. P. Newson, D. J. Richardson, and D. N. Payne, "Self-Starting Passively Mode-Locked Fiber Ring Soliton Laser Exploiting Nonlinear Polarization Rotation," *Electron. Lett.*, vol. 28, no. 15, pp. 1391-1393, Jul. 16 1992.
[10] U. Keller *et al.*, "Semiconductor saturable absorber mirrors (SESAM's) for femtosecond to nanosecond pulse generation in solid-state lasers," *IEEE J. Sel. Top. Quantum Electron.*, vol. 2, no. 3, pp. 435-453, 1996.
[11] D. J. Richardson, R. I. Laming, D. N. Payne, V. Matsas, and M. W. Phillips, "Self-Starting, Passively Modelocked Erbium Fiber Ring Laser Based on the Amplifying Sagnac Switch," *Electron. Lett.*, vol. 27, no. 6, pp. 542-544, Mar.14 1991.
[12] Z. W. Liu, Z. M. Ziegler, L. G. Wright, and F. W. Wise, "Megawatt peak power from a Mamyshev oscillator," *Optica*, vol. 4, no. 6, pp. 649-654, Jun. 2017.
[13] P. Sidorenko, W. Fu, L. G. Wright, M. Olivier, and F. W. Wise, "Self-seeded, multi-megawatt, Mamyshev oscillator," *Opt. Lett.*, vol. 43, no. 11, pp. 2672-2675, Jun. 2018.
[14] E. Ding, S. Lefrancois, J. N. Kutz, and F. W. Wise, "Scaling Fiber Lasers to Large Mode Area: An Investigation of Passive Mode-Locking Using a Multi-Mode Fiber," *IEEE J. Quantum Electron.*, vol. 47, no. 5, pp. 597-606, May 2011.
[15] R. Sidharthan *et al.*, "Ultra-low NA step-index large mode area Yb-doped fiber with a germanium doped cladding for high power pulse amplification," *Opt. Lett.*, vol. 45, no. 14, pp. 3828-3831, Jul. 2020.
[16] W. Liu *et al.*, "Femtosecond Mamyshev oscillator with 10-MW-level peak power," *Optica*, vol. 6, no. 2, pp. 194-197, Feb. 2019.
[17] R. H. Stolen and C. Lin, "Self-phase-modulation in silica optical fibers," *Phys. Rev. A*, vol. 17, no. 4, pp. 1448-1453, Apr. 1978.